Renewable Energy and Smart Systems Journal Vol. 2, No. 1, 2025: 30-39

Renewable Energy and Smart Systems

journal homepage: https://sanad.iau.ir/journal/res

Investigation of the causes and prevention of corrosion in the 11-megawatt electric motor of the Khatun Abad copper melt oxygen plant

Mohammad Jalal Shadman[1,*], Mahdiyeh Eslami[2], Mehdi Jafari Shahbazzadeh[2]

[1] *Senior Expert in Planning and Status Monitoring, Engineering Affairs, Shahre Babak Copper Complex, National Copper Industries Company of Iran. Shadman.mj61@gmail.com*

[2] *Department of Electrical Engineering, KeC, Islamic Azad University, Kerman, Iran*

Article info

Keywords:
Ozone, Nitric Acid, Partial Discharge, Corrosion, High Voltage, Ionization.

Article history:
Received: 25 01 2025
Accepted: 01 10 2025

Abstract

High-voltage electric motors are increasingly employed across industrial sectors due to rising energy demand and the expansion of energy-intensive processes. Given their high capital cost, complex operational conditions, and critical role in industrial continuity, improving efficiency and reliability is essential. Even minor degradation mechanisms can result in significant economic losses through unplanned downtime, reduced performance, and premature failure. One of the most critical degradation phenomena in high-voltage motors is partial discharge (PD), which occurs when localized electric fields exceed the dielectric strength of insulation systems, producing micro-scale electrical discharges. Partial discharge imposes combined thermal, chemical, and electrical stresses that progressively deteriorate insulation and surrounding components. In gas-cooled high-voltage motors, PD is often associated with ionization processes in cooling media such as air or hydrogen. A particularly harmful byproduct of PD is ozone, generated through oxygen ionization under strong electric fields. Ozone is a highly reactive oxidizing agent that accelerates corrosion of metallic components, degrades insulation materials, and ultimately reduces motor reliability. Despite its damaging effects, PD-induced ozone corrosion is frequently underestimated in industrial practice. Most previous studies on partial discharge and ozone effects have been limited to laboratory experiments or numerical simulations. In contrast, this research investigates the real operating conditions of an 11 MW high-voltage electric motor installed at the Khatun Abad Copper Smelting Oxygen Plant. Field observations and operational data analysis reveal clear links between partial discharge activity, ozone formation, and corrosion within the motor chamber and cooling components. These findings provide valuable insight into PD-related degradation mechanisms under actual industrial conditions. Based on the identified root causes, the study proposes practical mitigation strategies aimed at reducing PD activity and its consequences. These measures include optimization of the earthing system to lower electric field intensity and the controlled injection of compressed air to dilute ozone concentration and improve internal gas circulation. Furthermore, these technical solutions are integrated into a preventive maintenance (PM) strategy to enable early detection and long-term control of PD-related damage. The proposed approach offers directly applicable solutions for enhancing the reliability, safety, and service life of high-voltage motors in industrial environments.

* Corresponding author
E-mail address Shadman.mj61@gmail.com (M.J Shadman)

1. Introduction

Electrical corrosion is a serious challenge in the electrical industry and power systems, as it can significantly reduce the operational lifespan of electrical equipment, particularly high-voltage electric motors. This type of corrosion can markedly affect the efficiency, longevity, and safety of such equipment. In various industries, including the production of gases like oxygen, electric motors function as the primary drivers in energy production and transmission processes. Therefore, maintaining the optimal performance of these motors is of critical importance. One of the primary causes of corrosion in high-voltage electric motors is the phenomenon of corona electrical discharge. This phenomenon typically occurs under conditions of high voltages and intense electric fields, and it can lead to the degradation of insulation and the internal components of the motor. In oxygen production plants, which are often exposed to specific environmental conditions and fluctuating temperatures, the risks associated with electrical corrosion become more pronounced. This paper investigates the causes and contributing factors of corrosion in an 11-megawatt electric motor at the Khatun Abad Copper Smelting Oxygen Plant. In this facility, a three-stage centrifugal compressor is used to produce compressed air for the process of separating its constituent components, including oxygen and nitrogen. The main driving force of the compressor is an electric motor with a capacity of 11 MW and a rated voltage of 10 kV, which is cooled by a cooler equipped with two heat exchangers. The study analyzes the impact of corrosion on the performance and operational lifespan of the motor. Additionally, the paper will propose strategies to prevent this type of corrosion and enhance the efficiency and safety of the equipmen. The aim of this study is to raise awareness of the risks of electrical corrosion and to improve maintenance and repair practices in industries related to oxygen production. Online partial discharge (PD) testing has been widely applied to rotating machines above 6 kV since the late 1980s. PD monitoring is a powerful tool for providing evidence of winding insulation degradation months or even years in advance, enabling the planning of appropriate corrective maintenance actions and thereby preventing unexpected in-service failures. PD is typically the primary indicator of fault mechanisms in stator windings. By analyzing these signals, the root cause can be inferred. However, there are circumstances in which PD itself is the cause, for example, when discharges lead to the formation of ozone inside a sealed device. The presence of ozone can result in the formation of nitric acid (HNO_3), a highly corrosive substance that attacks not only insulating materials but also the metallic components of the device. This paper presents a case study of a synchronous motor in which very high PD levels were detected, leading to an internal inspection and confirmation of damage, likely caused by the chemical attack of nitric acid on various parts of the machine. The most severe problem may be observed in the rotor, where cracks and gaps in the damper winding cage could have been caused or exacerbated by this acid [1].

This section addresses the selection of insulation systems for use in new machines and details over thirty different failure mechanisms of rotor and stator windings, including methods for repair or, at a minimum, slowing down each failure process. Finally, it reviews the theoretical foundations, practical applications, and interpretation of forty different tests and monitoring techniques used to assess the condition of winding insulation, thereby helping machine operators prevent unnecessary failures and reduce maintenance costs [2].

This paper provides a review of the insulation design of electrical machines, techniques and methods for modeling and testing insulating materials, and recent advancements in this field. Several testing standards and methods for detecting insulation failure are discussed. Case studies of insulation failures in electrical machines are presented to direct the reader's attention toward a more practical, real-world approach. Issues related to high-voltage insulation systems used in industries such as aerospace power plants, hydroelectric generators, and wind turbine generators are discussed in this paper. Partial discharge monitoring techniques are reviewed, and their implications in most high-voltage aerospace applications as well as emerging advanced applications are examined. Finally, polymer nanocomposite materials with exceptional dielectric strength or thermal conductivity are highlighted as a promising outlook for the future of insulation design in electrical machines [3].

Stator winding insulation failure is one of the most frequent causes of stator winding faults, leading to forced outages of medium-voltage (MV) motors. This paper presents case studies of 15 stator winding insulation failures in MV motors supplied from the grid, which occurred between 2011 and 2015 in the pulp and paper, power generation, and petrochemical industries. The insulation failures are analyzed based on the design of the insulation system, motor operating conditions, fault location, and the motor failure pattern. The inspection and testing records of the stator insulation, including insulation resistance (IR), polarization index (PI), leakage current, dissipation

factor, and partial discharge (PD) tests, are also presented for the failed motors. Insights are provided on how stator winding insulation failures can be prevented, based on the analysis of past failures [4].

This paper proposes a simple and robust sensorless method for online detection of stator winding faults by observing an off-diagonal element of the sequence impedance matrix. Given the destructive nature and rapid propagation of insulation failures, early detection of winding faults is crucial to prevent further damage to the motor. Motor non-idealities, such as variations in supply voltage imbalance, slip-dependent effects of the motor's inherent asymmetry, and measurement errors, must be taken into account to reliably detect a winding fault at its early stage. For reliable early-stage detection of winding faults, motor non-idealities such as variations in supply voltage imbalance, slip-dependent effects due to inherent motor asymmetries, and measurement errors must be thoroughly considered. Simulation and experimental results on a 5-horsepower induction machine are presented to validate the proposed method. It has been demonstrated that the proposed rotor fault detection scheme is simple and capable of providing fault diagnosis that is resilient to motor non-idealities [5].

Calculations and voltage application experiments on a test cell simulating a high-resistance conduction path in series with a cavity within polyethylene are discussed. These experiments caused chemical modifications on the surfaces of the cavities for both current types: currents produced by voltages below the initial critical threshold and corona currents within the different cavities. X-ray photoelectron spectroscopy (XPS) of the chemical species on the cavity surface reveals similar components (functional groups), indicating that the currents or discharges induce degradations analogous to those observed in corona insulation failures. X-ray photoelectron spectroscopy (XPS) of the chemical species on the cavity surface reveals similar components (functional groups), indicating that the current or discharge induces damage similar to that seen in corona insulation failures. The longer time required for the growth of sub-corona species aligns with the occurrence of breakdowns over periods ranging from several months to a few years. Favorable electric field conditions for the presence of sub-corona currents have been established at relatively low voltages [6].

Previous studies have documented the behavior of partial discharge (PD) in varnish-coated motor windings under sub-atmospheric pressure conditions, using repetitive square and sinusoidal voltage waveforms. The objective of this research is to investigate whether monitoring partial discharge in commercial aircraft actuators is feasible. The findings indicate that detecting partial discharge using UHF techniques is achievable for aircraft operating at altitudes below 10 kilometers. It was also found that, for varnished windings, the lower discharge voltage predicted by the Paschen curve provides a conservative estimate of the inception voltage for partial discharge and, therefore, can serve as a basis for insulation system design. [7] The rapid growth of electrical devices in More Electric Aircraft (MEA) drives an increased demand for higher electrical power. This, in turn, necessitates higher voltages, which increase the electrical stress on the insulation system. This can lead to partial discharge (PD) in the aircraft insulation system. Additionally, the aircraft generator supplies electrical power at variable frequencies. As a result, the aircraft generator's insulation system experiences a range of electrical stresses under varying voltage frequencies. Under these conditions, there is a strong interest in partial discharge detection. This paper presents experimental tests conducted to study the effect of voltage frequency and air pressure on the characteristics of corona PD pulses [8] Partial discharge (PD) is a phenomenon that often occurs in insulation system defects (cavities), which can significantly affect the equipment's lifetime and reliability. While extensive knowledge has been gained on the phenomenology of PD in high-frequency transformer (HFT) systems under sinusoidal AC voltage, much less work has been done to deduce PD behavior under high-frequency pulse-width modulation (PWM) operating conditions. One major barrier has been the limitation of suitable testing equipment. A new high-frequency ±5 kV GaN PWM source with controllable dV/dt, voltage level, and frequency has been developed. This paper explores the application of these measurements for testing materials under such electrical environments. Two windings, commonly used for HFTs, were tested under varying applied voltages, frequencies, and slew rates. Based on the experimental results, at high frequencies (up to 50 kHz), the electric field generated by space charge deposited from PD occurring during previous PWM pulses plays a significant role in PD behavior. The frequency-dependent permittivity of the insulating material can also influence the PD measurement results [9].

A fundamental research program was initiated to explore the use of silica nanotechnology for improving the electrical and mechanical properties of stator winding insulation in generators. When the new SiO_2 nanocomposite insulation was tested in 0.6-meter-long tubular samples with the original mica-epoxy

insulation system, it exhibited an electrical life curve with a gentler slope compared to conventional winding insulation, leading to a significant improvement in lifespan under both nominal and operational electrical stresses. As the next stage of development, the original stator bars with standard design parameters for hydro generators were manufactured. Voltage endurance tests were conducted at various stress levels to obtain electrical life curves. Initial results indicate a longer lifespan for the nanocomposite compared to the conventional insulation system. The incorporation of SiO_2 nanoparticles into the mica-epoxy insulation results in a more efficient stator winding insulation system, which on one hand enhances the specific output power and on the other hand is designed to meet the highly flexible requirements of modern grids without compromising lifespan [10].

This paper evaluates the feasibility of using the stator resistance estimate (R_s) as an indicator of the stator winding temperature (T_s). The advantages of resistance-based temperature monitoring over conventional thermal model-based methods are presented. Since obtaining an accurate estimate of R_s is critical for this approach, existing R_s estimation schemes are reviewed, along with an analysis showing the sensitivity of model-based R_s estimates due to uncertainties in motor parameters and variables. It has been shown that estimating R_s during high-speed operation is challenging, as the estimated R_s becomes sensitive to errors in motor parameters and electrical variables when the frequency (speed) of the input excitation increases. A new R_s estimation scheme is proposed for temperature monitoring under steady-state conditions. Experimental results on a line-connected induction machine validate the proposed method and its analysis [11].

A new online technique for monitoring the insulation condition of AC machine stator windings is proposed in this paper. The approach is based on non-invasively measuring the differential leakage currents of each winding phase from the terminal box, enabling the assessment of insulation condition during motor operation [12].

Conventional differential CTs used for phase-fault protection can be replaced with high-performance current sensors to measure leakage currents with higher accuracy. Insulation condition indicators, such as capacitance and dissipation factor, are derived from these measurements to provide a low-cost solution for online insulation monitoring. A simplified online insulation system model is developed for analyzing and interpreting the measured data. Experimental results on a 15 hp induction motor under simulated insulation degradation conditions show that the proposed method is highly sensitive and capable of detecting early signs of insulation deterioration. Conventional differential CTs used for phase fault protection can be replaced with high-performance current sensors to achieve more accurate leakage current measurements. Key insulation health indicators—such as capacitance and dissipation factor—are then computed from these measurements, offering a cost-effective approach for real-time insulation condition assessment. A simplified online insulation system model is formulated to facilitate the analysis and interpretation of the acquired data. Experimental validation on a 15-horsepower induction motor, under simulated insulation degradation, confirms that the proposed method is highly sensitive and capable of detecting early-stage insulation deterioration [12].

The measurement of the dissipation factor (e.g., tan δ) and insulation capacitance (IC) are conventional monitoring methods for assessing the aging level of insulation systems. These values provide valuable indications of dielectric losses in insulating materials. However, the way in which these values are affected by aging processes caused by thermal stresses has, to date, never been fully investigated. Therefore, this study demonstrates the influence of thermal aging on tan δ and IC of windings for electrical machines (EMs). The work is carried out for class 200 round enameled magnet wire samples. The aim of this study is to improve the EM design process for short-duty-cycle applications. Hence, the outcome may be incorporated into the design stage to enhance reliability and lifespan. Random windings are chosen in the conducted study, as they are the most common winding arrangement for low-voltage EMs used in a wide range of applications (e.g., from household appliances to aerospace motors). Based on the collected data, considerations regarding the influence of relative humidity on both the dissipation factor and IC are presented. Finally, the correlation between the partial discharge inception voltage and the diagnostic measurements is experimentally confirmed [13].

Mica sheets are a vital component of electrical machine insulation. Although considerable attention has been given to partial discharges and their deteriorating effect on such insulation, relatively little attention has been paid to surface discharges. This paper examines the effect of water droplets—their volume, conductivity, position, and quantity—on the flashover voltage of mica sheets. It has been shown

that all of the aforementioned parameters affect the flashover voltage [14].

Measuring the partial discharge inception voltage (PDIV) under repetitive impulse voltages should be performed on the insulation of low-voltage inverter-fed motors to ensure that the rated voltages are lower than the PDIV, thereby preventing partial discharges (PD) from occurring in the insulation systems. Given that PD signals from the test objects and the interference generated by the impulse voltage generator often exhibit similar characteristics in both the time and frequency domains, ultra-high frequency (UHF) technologies are recommended for use under repetitive impulse voltage conditions. This is because UHF sensors (combined with high-frequency filters) with suitable bandwidth can detect PD signals and effectively suppress interference. However, PD tests using UHF under impulse voltages have the following limitations: (1) The sensitivity of UHF sensors is significantly lower compared to conventional PD testing methods under sinusoidal voltages. (2) The signal-to-noise ratio (SNR) during PD testing under impulse voltages with very fast rise times (e.g., 50 ns) is not sufficient. To address the above issues, the aim of this paper is to investigate improvements when performing PDIV tests under very fast rise-time impulse voltages, including designing a new UHF sensor specifically for PD and PDIV tests under repetitive impulse voltages, determining a reasonable distance between the UHF sensor and the test object, and proposing a new method during PDIV testing using Assisted Trigger software on the oscilloscope to prevent interference-triggered excitation and to capture the first PD pulse [15].

2- Corona Phenomenon

Corona essentially refers to the ionization of nitrogen in the air and occurs when the electric field intensity around conductors exceeds a critical threshold, leading to partial discharges in the gaseous environment. This type of discharge appears as electrical sparks or blue glow, typically observable near high-voltage conductors. The intensity of these discharges increases under high-voltage conditions and is influenced by environmental factors such as humidity, surface contamination, and temperature. In this study, the occurrence of corona in the 11 MW electric motor at the Khatunabad Oxygen Plant was documented and linked to internal partial discharges within the motor. These discharges caused internal component corrosion and ozone generation in the cooling chambers. A combined analysis of corona and partial discharges demonstrates the direct role of these processes in reducing motor reliability and inducing internal damage, filling a research gap in previous studies.

2-1 Critical Voltage

The minimum voltage that causes electrical breakdown in an insulation, resulting in the loss of its dielectric properties, is called the critical voltage gradient. The voltage that produces this critical gradient is referred to as the critical voltage.

2- 2 Visible Corona Voltage

When the line voltage reaches the critical level, ionization initiates in the air adjacent to the conductor surface. At this stage, however, the corona phenomenon is not yet observable. For visible corona to occur, the electrons must attain sufficiently high velocities upon colliding with atoms and molecules, necessitating an even higher voltage. Corona can also develop in low-pressure discharge tubes subjected to high potential differences, as used in plasma generation. In such cases, the gas undergoes corona discharge prior to complete electrical breakdown. This phenomenon occurs exclusively at locations with concentrated electric fields, such as sharp edges or surface imperfections, where the surrounding gas becomes conductive, forming a luminous halo. This process is also commonly referred to as unipolar discharge. The most prominent indication of corona is the appearance of a luminous glow surrounding high-voltage conductors. Corona is essentially the ionization of atmospheric nitrogen, and the associated energy losses manifest as light and heat around the conductor surface. The visual manifestation of corona includes light, whose wavelength varies from infrared to ultraviolet depending on the intensity of the discharge. Other indicators include the audible sound of small electrical sparks, the formation of ozone (detectable by its characteristic smell in the surrounding environment), and the production of nitric acid resulting from the reaction of ionized nitrogen with moisture in the air, which appears as a white mist around the conductors [16, 17].

3- Ozone

Partial discharge (PD) occurring on the surface of a winding or busbar induces chemical reactions in the surrounding air. One of the byproducts of these reactions is ozone, a gas with a distinct odor. When significant PD activity is present, the concentration of ozone in the environment increases. Ozone is recognized as one of the most powerful oxidizing

agents, considerably stronger than O_2. Its half-life varies depending on atmospheric conditions such as temperature, humidity, and air movement. If a fan causes ozone circulation in an insulated environment, its half-life at room temperature is approximately one day. Some scientific sources estimate the ozone half-life under atmospheric conditions to be around thirty minutes.

3-1 Ozone and Metals

Ozone oxidizes most metals to their highest oxidation states. However, gold, platinum, and iridium do not follow this rule. For example, the oxidation reaction of copper is shown below [18].

$$Cu + O_3 \rightarrow CuO + O_2 \quad (1)$$

3-2 Reaction with Nitrogen and Carbon Compounds

Ozone oxidizes nitric oxide (NO), converting it into nitrogen dioxide (NO_2):

$$NO + O_3 \rightarrow NO_2 + O_2 \quad (2)$$

Nitrogen dioxide also participates in oxidation reactions again, resulting in the formation of NO3, which in further reaction with nitrogen dioxide, converts to N2O5. The various reactions of ozone with nitrogen and carbon compounds are presented below: [A18]

$$NO_2 + O_3 \rightarrow NO_3 + O_2 \quad (3)$$
$$NO_2 + ClO_2 + 2O_3 \rightarrow NO_2ClO_4 + 2O_2$$
$$2NH_3 + 4O_3 \rightarrow NH_4NO_3 + 4O_2 + H_2O$$

3-3 Reaction with Sulfur Compounds

Ozone acts as an oxidizing agent, transforming sulfides into sulfate.

$$PbS + 4O_3 \rightarrow PbSO_4 + 4O_2 \quad (4)$$

With the aid of water, sulfur or sulfur dioxide, and ozone, sulfuric acid can be obtained.

$$S + H_2O + O_3 \rightarrow H_2SO_4 \quad (5)$$
$$3SO_2 + 3H_2O + O_3 \rightarrow 3H_2SO_4$$

In the gas phase, ozone reacts with hydrogen sulfide to produce sulfur dioxide.

$$H_2S + O_3 \rightarrow SO_2 + H_2O \quad (6)$$

In an aqueous solution, two reactions occur simultaneously: one leads to the formation of sulfur, while the other results in the production of sulfuric acid.

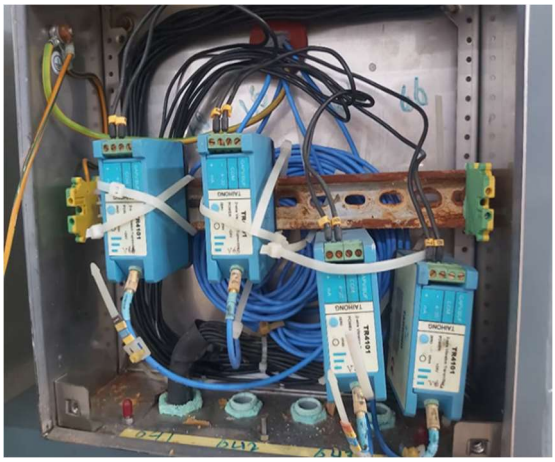

Figure 1: Corrosion in the electric motor instrumentation panel.

$$H_2S + O_3 \rightarrow S + O_2 + H_2O \quad (7)$$
$$3H_2S + 4O_3 \rightarrow 3H_2SO_4$$

4- Destructive Effects

Ozone gas attacks any type of polymer that includes double bonds in its carbon chain. Rubber products such as latex, nitrile rubber (NBR), and styrene-butadiene rubber (SBR) are susceptible to ozone attacks. As a result of these attacks, cracks appear on the surface of these polymers, which increase in depth and width over time. The extent of this degradation depends on the concentration of ozone in the atmosphere and the load (weight) borne by the rubber. These types of rubber are protected against ozone degradation with the help of “antiozonant” materials, such as wax. Rubber gaskets and O-rings, which play

Figure 1: Corrosion in the electric motor instrumentation panel.

near direct current electric motors increases ozone cracking because the commutator of these motors generates sparks during operation, which are effective in producing ozone gas [18].

5- Influential observations for investigating the factors causing degradation

5-1 Observation of Corrosion

With the commencement of operation at the oxygen plant, signs of corrosion began to appear on the

Figure 2: Corrosion in the electric motor power panels.

precision instruments installed within the electric motor panels after a short period, causing serious damage to this equipment. To analyze the current situation and gather more information, an inspection of the interior of the panels was conducted, and photographs of the corrosion on the electrical equipment were taken, as shown below. Figures (1 and 2)

Initially, due to the presence of an unpleasant odor in the factory environment, the existence of SO_2 was suspected, which led to the analysis of the air surrounding the electric motor (Table 2). The results indicated that the SO_2 concentration was within the normal range (<1 ppm). Consequently, suspicions shifted toward the presence of ozone in the factory environment.

As an initial step to identify ozone-induced corrosion, the mercury test was employed. In this method, liquid mercury was exposed to the air around the electric motor, and the effect of ozone was observed as a thin layer of deposit forming on the mercury surface.

As illustrated in Figures 1 and 2, corrosion is observed in various parts of the electric motor. Considering the critical importance of the motor in the oxygen production process, further investigation and resolution of this issue have been undertaken, as detailed below.

6-Investigation and Results:

1. Investigation of the gas emitted from the electric motor housing and its effects on water properties (details provided in Activity Description, Item 1) (Figure 3).
2. Analysis of the Grounding System of the Electric Motor and the Oxygen Plant, and the Proposed Modifications to the Existing System

Figure 4: Examination of the electric motor grounding system and the presence of circulating currents

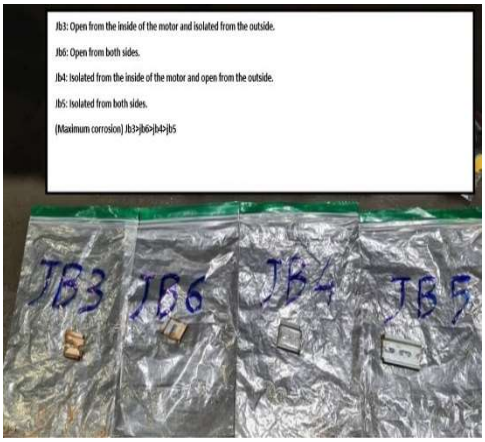

Figure 5: Available samples of corrosion on

Description of Activities Performed (Section 2) (details provided in Activity Description, Item 3) (Figure 4).

3. Examination of Existing Samples of Component Corrosion (Figures 5, 6, and 7)
4. Disassembly of the Electric Motor Cooler, Cleaning, and Restoration of the Insulation Coating

Figure 6: Presence of corrosion on the elastic rubber components

Figure 7: Corrosion of parts of the cooling cooler

7-Description of Activities Conducted

To investigate the type of gas emitted from the electric motor, in addition to the initial mercury test, two further experiments were designed and carried out, as described below (Figure 3). First experiment: Initially, 800 mL of demineralized water was prepared, and its pH and electrical conductivity were measured. The initial pH was recorded as 7.49, and the initial electrical conductivity was 1.52 µS/cm. Subsequently, the water was exposed for 72 hours to the gas released from the motor housing via the drainage outlet of the water leakage detection switch. The results revealed a significant drop in pH to 1.95, accompanied by a substantial increase in electrical conductivity. These findings clearly indicate that the emitted gas is acidic in nature. In the second experiment: To identify the constituent molecules of the air inside and outside the electric motor housing, an analysis of the air was performed. The results revealed that the concentration of ozone inside the motor housing was higher than that of the surrounding ambient air. This indicates that the electric motor generates ozone gas. (Tables 1 and 2)

Table 1: Analysis of Air Inside the Electric Motor Chamber

Row	Station	Parameter	Unit	Results
1	Output 1	Ozone	ppm	0.18
2	Output 2			0.37

1. Considering that the grounding system of the oxygen plant is a rod-bonded configuration, and based on the measurements performed, the system's resistance does not meet the required standard, with the measured value being approximately 40 ohms. Moreover, due to the presence of circulating currents in the bonding loops—caused by the high resistance of the plant's grounding system—these currents are discharged through the outer casing of the electric motor.
2. The preventive maintenance (PM) program for the existing electric motor, following the proposed condition monitoring measures, was developed with the following activities:

a- Periodic Activities:

- ✓ Measurement of the pH of the test water every 72 hours.
- ✓ Daily inspection of the instrument air flow rate, ensuring it remains within the permissible limit of 3 Nm^3/min.
- ✓ Monthly inspection of electrical and instrumentation boxes.
- ✓ Quarterly analysis of the gases emitted from the electric motor housing.

b- Major Overhaul Program:

- ✓ Opportunistic/overhaul maintenance, including:
- ✓ Disassembly and servicing of the cooling unit.
- ✓ Leakage testing of the cooler.

Table 2: Analysis of the outdoor air environment of the electric motor

Row	Factor	Unit	Value
1	PM 1	µg/m³	6
2	PM 2.5	µg/m³	12
3	PM 4	µg/m³	33
4	PM 7	µg/m³	46
5	PM 10	µg/m³	61
6	TSP	µg/m³	91
7	CO2	ppm	389
8	O2	%	20.9
9	CO	ppm	0.51
10	SO2	ppm	0.137
11	SO3	ppm	0.018
12	H2SO4	ppm	0.014
13	HF	ppm	< 0.001
14	HCl	ppm	< 0.001
15	N2	%	78.04

8- Conclusion:

The experiments and investigations revealed that the primary cause of corrosion on various parts of the 11 MW oxygen plant electric motor was the generation of ozone gas, resulting from the ionization of the air inside the motor housing. This phenomenon is caused by electric current leakage (Corona discharge). In this case, negative charges adhere to the sharp edges of components, leading to corrosive effects. Additionally, due to its strong oxidizing properties, ozone causes significant degradation to resilient rubber components and rubber clamps. Considering that the retention time of ozone gas inside the motor housing is approximately 30 minutes, the injection of instrument air—containing only oxygen and nitrogen—into the plant prevented the persistence of ozone during this period. Moreover, eddy currents on the motor casing were significantly reduced by restoring the grounding system to an optimal condition. These findings, in addition to identifying the primary cause of corrosion, have a direct impact on improving maintenance and operational strategies for high-voltage motors. Implementing similar approaches in related industries can enhance equipment reliability, reduce internal damage, and extend the operational lifespan of electric motors.

References

[1] G. L. Cestaro and M. F. Fernandes, "Fault detection in components of synchronous motors through online partial discharge measurements," IEEE Petroleum and Gas Conference, 2024. [Online]. Available: https://ieeexplore.ieee.org

[2] G. C. Stone, I. Culbert, E. A. Boulter, and H. Dhirani, Electrical Insulation for Rotating Machines: Design, Evaluation, Aging, Testing, and Repair, 1st ed. London, UK: IET, 2014.

[3] H. Raziq, M. Batool, F. Nawaz, A. Akgül, F. Fzal, and M. K. Hassani, "A review on analysis and modeling of electrical machine insulation system," Journal Name, Article 2400614, Feb. 12, 2024, Accepted Aug. 31, 2024, Published online Sep. 12, 2024.

[4] S. Bin Lee, T.-J. Kang, H. Kim, T. Kong, and C. Lim, "Case studies of stator winding turn insulation failures in medium voltage motors," in 2017 Annual Pulp, Paper and Forest Industries Technical Conference (PPFIC), pp. 1–8, 2017.

[5] S. Bin Lee, R. M. Tallam, and T. G. Habetler, "A robust, on-line turn-fault detection technique for induction machines based on monitoring the sequence component impedance matrix," IEEE Trans. Power Electron., vol. 18, no. 3, pp. 865–872, 2003, doi: 10.1109/TPEL.2003.810848.

[6] A. M. Bruning, D. G. Kasture, F. J. Campbell, and N. H. Turner, "Effect of cavity sub-corona current on polymer insulation life," IEEE Trans. Electr. Insul., vol. 26, no. 4, pp. 826–836, 1991, doi: 10.1109/14.83709.

[7] A. Cavallini, L. Versari, and L. Fornasari, "Feasibility of partial discharge detection in inverter-fed actuators used in aircrafts," in 2013 Annual Report Conference on Electrical Insulation and Dielectric Phenomena, pp. 1250–1253, 2013.

[8] A. N. Esfahani, S. Shahabi, G. Stone, and B. Kordi, "Investigation of corona partial discharge characteristics under variable frequency and air pressure," in 2018 IEEE Electrical Insulation Conference (EIC), pp. 31–34, 2018, doi: 10.1109/EIC.2018.8481047.

[9] Z. Guo, A. Q. Huang, R. E. Hebner, G. C. Montanari, and X. Feng, "Characterization of partial discharges in high-frequency transformer under PWM pulses," IEEE Trans. Power Electron., vol. 37, no. 9, pp. 11199–11208, 2022, doi: 10.1109/TPEL.2022.3169747.

[10] T. Hildinger and J. R. Weidner, "Progress in development of a nanocomposite stator winding insulation system for improved generator performance," in 2017 IEEE Electrical Insulation Conference (EIC), pp. 139–142, 2017, doi: 10.1109/EIC.2017.8004655.

[11] S.-B. Lee, T. G. Habetler, R. G. Harley, and D. J. Gritter, "An evaluation of model-based stator resistance estimation for induction motor stator winding temperature monitoring," IEEE Trans. Energy Convers., vol. 17, no. 1, pp. 7–15, 2002, doi: 10.1109/60.986431.

[12] S. B. Lee, K. Younsi, and G. B. Kliman, "An online technique for monitoring the insulation condition of AC machine stator windings," IEEE Trans. Energy Convers., vol. 20, no. 4, pp. 737–745, 2005, doi: 10.1109/TEC.2005.853760.

[13] V. Madonna, P. Giangrande, and M. Galea, "Evaluation of strand-to-strand capacitance and dissipation factor in thermally aged enamelled coils for low-voltage electrical machines," IET Sci., Meas. Technol., vol. 13, no. 8, pp. 1170–1177, 2019, doi: 10.1049/iet-smt.2019.0071.

[14] S. Masloughkas and M. G. Danikas, "Study of water droplets behavior on electrical machine insulation under the influence of uniform electric fields: The influence of some parameters on mica sheets," Eng. Technol. Appl. Sci. Res., vol. 8, no. 1, pp. 2351–2355, 2018, doi: 10.48084/etasr.1691.

[15] P. Wang, W. Zhou, Z. Zhao, and A. Cavallini, "The limitation of partial discharge inception voltage tests at repetitive impulsive voltages using ultra-high frequency antenna and possible solutions," in 2018 IEEE Electrical Insulation Conference (EIC), pp. 192–195, 2018.

[16] H. Mohseni, Advanced High Voltage Engineering, Tehran, Iran: Publications and Printing Institute of Tehran University, 1994.

[17] M. Soltani, Power Plant Equipment, Tehran, Iran: Publications and Printing Institute of Tehran University, 1995.

[18] S. Bahar Kazemi, "Title of article," Faradars Journal, Jan. 15, 2023. [Online]. Available: https://b.fdrs.ir/1wu